

1  
2 **Supporting Information**

3  
4 **Benzylphosphonic Acid treated Ultra-thin ALD-InOx for**  
5 **Long term Device Stability**

6  
7 **Ju-Hun Lee<sup>a,b</sup>, Jaehyun Moon<sup>a,b</sup>, Kitae Kim<sup>c,e</sup>, Yeonjin Yi<sup>e</sup>, Soohyung park<sup>c,d</sup>, Jong-**  
8 **Heon Yang<sup>a</sup>, Chi-Sun Hwang<sup>a</sup>, and Seung-Youl Kang<sup>a\*</sup>**

9  
10  
11 <sup>a</sup> Reality Devices Research Division, Electronics and Telecommunication Research Institute  
12 (ETRI), Daejeon 34129, Republic of Korea

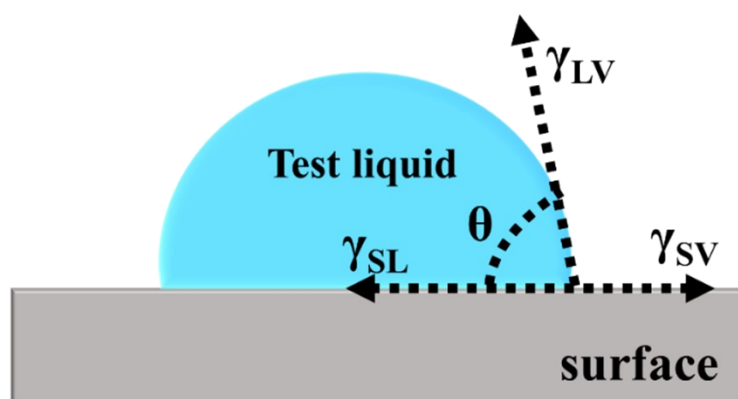
13 <sup>b</sup> Advanced Device Technology, ICT, University of Science and Technology (UST), Daejeon  
14 34113, Republic of Korea

15 <sup>c</sup> Advance Analysis & Data Center, Korea Institute of Science and Technology (KIST), Seoul  
16 02792, Republic of Korea

17 <sup>d</sup> Division of Nano & Information Technology, KIST School, University of Science and  
18 Technology (UST), Seoul 02792, Republic of Korea

19 <sup>e</sup> Department of Physics and van der Waals Materials Research Center, Yonsei University, 50  
20 Yonsei-ro, Seodaemun-gu, Seoul 03722, Republic of Korea

21  
22 \* Corresponding author e-mail: [kang2476@etri.re.kr](mailto:kang2476@etri.re.kr)  
23  
24  
25  
26  
27  
28  
29  
30  
31



32  
33  
34  
35  
36  
37  
38  
39  
40  
41

42 **Fig. S1.** Schematic of the CA depiction.  $\gamma_{SL}$  is the interfacial energy between the solid (S) and  
43 liquid (L),  $\gamma_{SV}$  is the SE the S-vapor (V),  $\gamma_{LV}$  is the SE. The SE L-V, and theta ( $\theta$ ) is the CA of  
44 the test liquid on the solid surface.

45  
46  
47  
48  
49  
50  
51  
52  
53  
54  
55

In general, for CA and SE, it has been useful to analyze between solid surfaces and other materials such as films. So, this system provides a wealth of information that can be used to interpret surface/interface properties. From this perspective, to investigate the SE, the CA method was used to confirm the change from hydrophilic to hydrophobic on the surface of untreated  $\text{In}_2\text{O}_3$  film and BPA- $\text{In}_2\text{O}_3$  film. As shown schematically in Figure S1, the CA testing method appears to be a simpler option when compared to other characterization methods such as electrical and optical testing

56 **Table 1.** Surface energy (SE) components of the test liquid with polar and dispersive SE

Test liquid	Tension ( $\text{mJ}/\text{m}^2$ )	Dispersive ( $\text{mJ}/\text{m}^2$ )	Polar ( $\text{mJ}/\text{m}^2$ )
Deionized water (DI)	72.8	22.5	50.3
Ethylene glycol (EG)	48.3	39.3	19

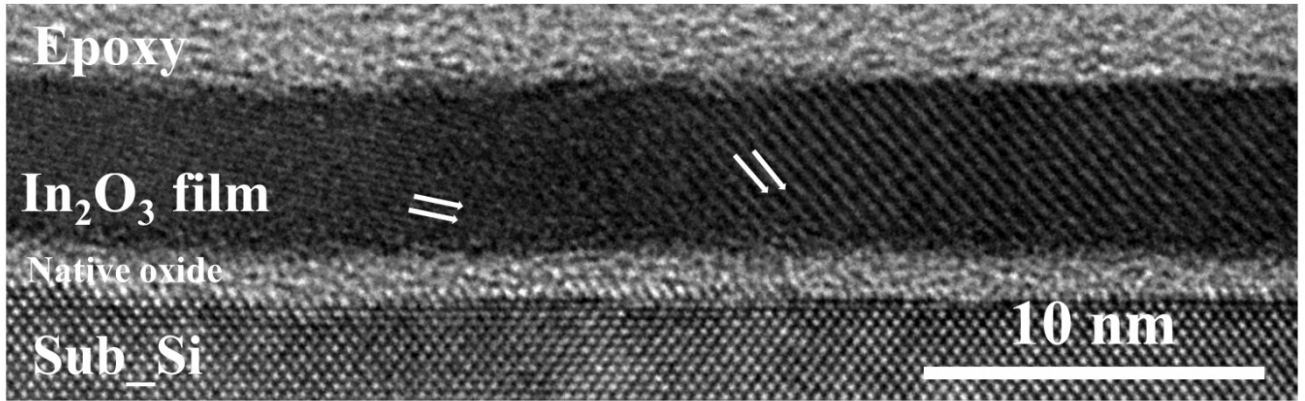
60  
61  
62  
63

**Table S1.** The test liquid parameter values used here for polar and non-polar liquids.

64 As shown the Table S1, the conventional testing liquid with different polar and dispersive  
65 components is used for testing. The polar and dispersive SE components of the two test liquids  
66 used in the study. To interpret the SE from the acquired CA data acquisition, it used to the  
67 owens-wendt method (OW) equation method. The polar and non-polar testing liquids were  
68 used the DI and EG, respectively. The OW models obtained information about the trend of SE

69 as the surface changes from hydrophilic to hydrophobic temporal for untreated  $\text{In}_2\text{O}_3$  and BPA-  
70  $\text{In}_2\text{O}_3$  films.

71



72

73

74

75

76

77

78

79

80

81

82

83

84

85

86

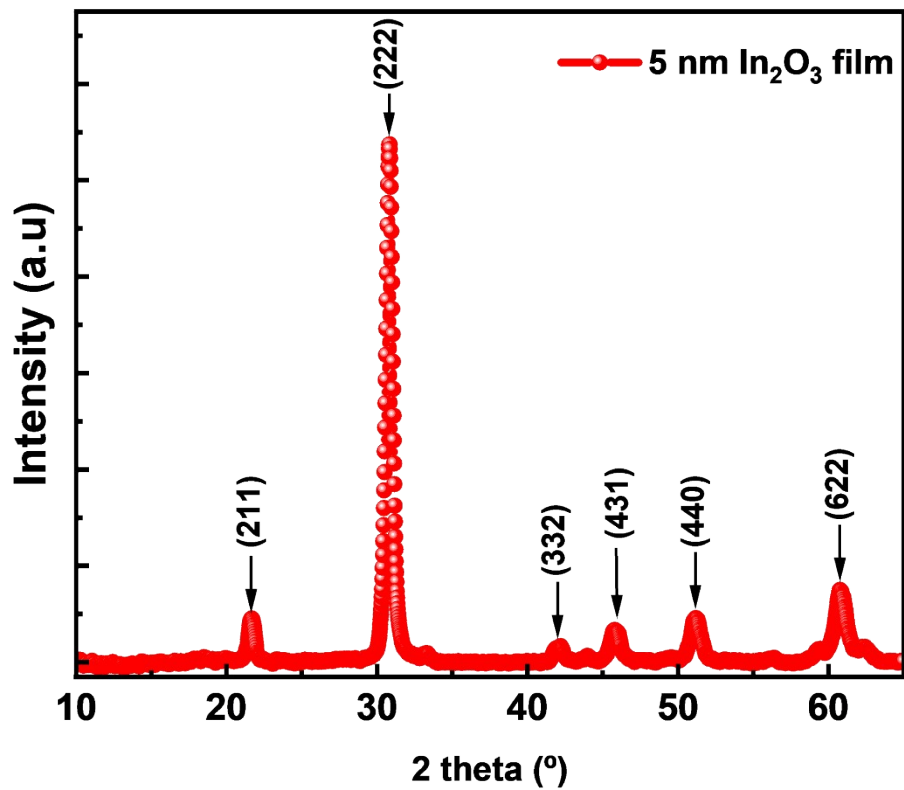
87

88

89

90

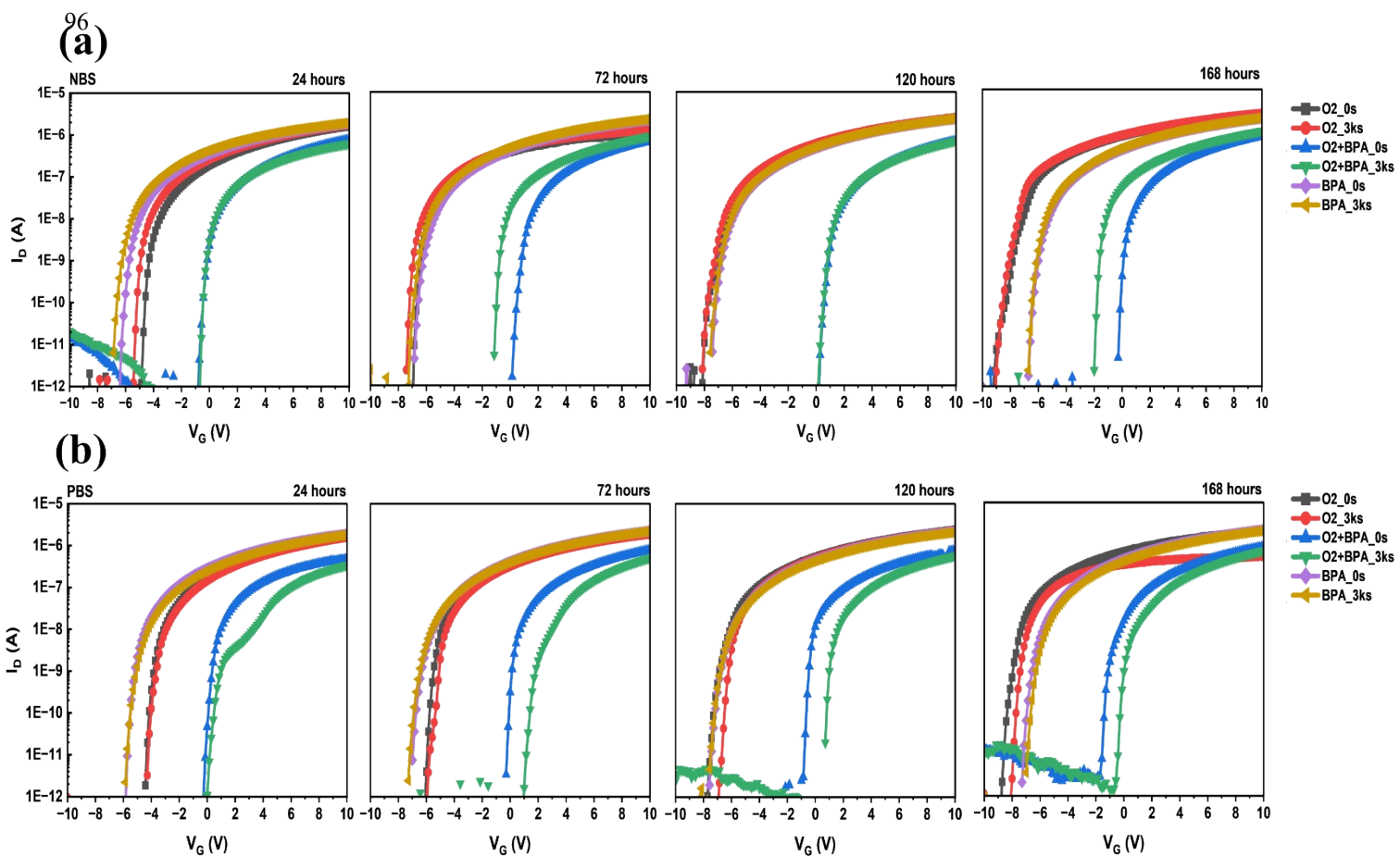
91



92 **Fig. S2.** The top image shows a TEM cross-section of a 5 nm polycrystalline  $\text{In}_2\text{O}_3$  film. the  
93 bottom image shows the XRD peak information of the  $\text{In}_2\text{O}_3$  film.

94

95



97

98 **Fig. S3.** The transfer curve of the 5 nm  $\text{In}_2\text{O}_3$  TFT was analyzed under negative (a) and positive  
 99 bias stress (b) (NBS, PBS) at  $V_G$  of  $\pm 5$  V over a period of 168 hours.

100

101

102

103

104

105

106

107

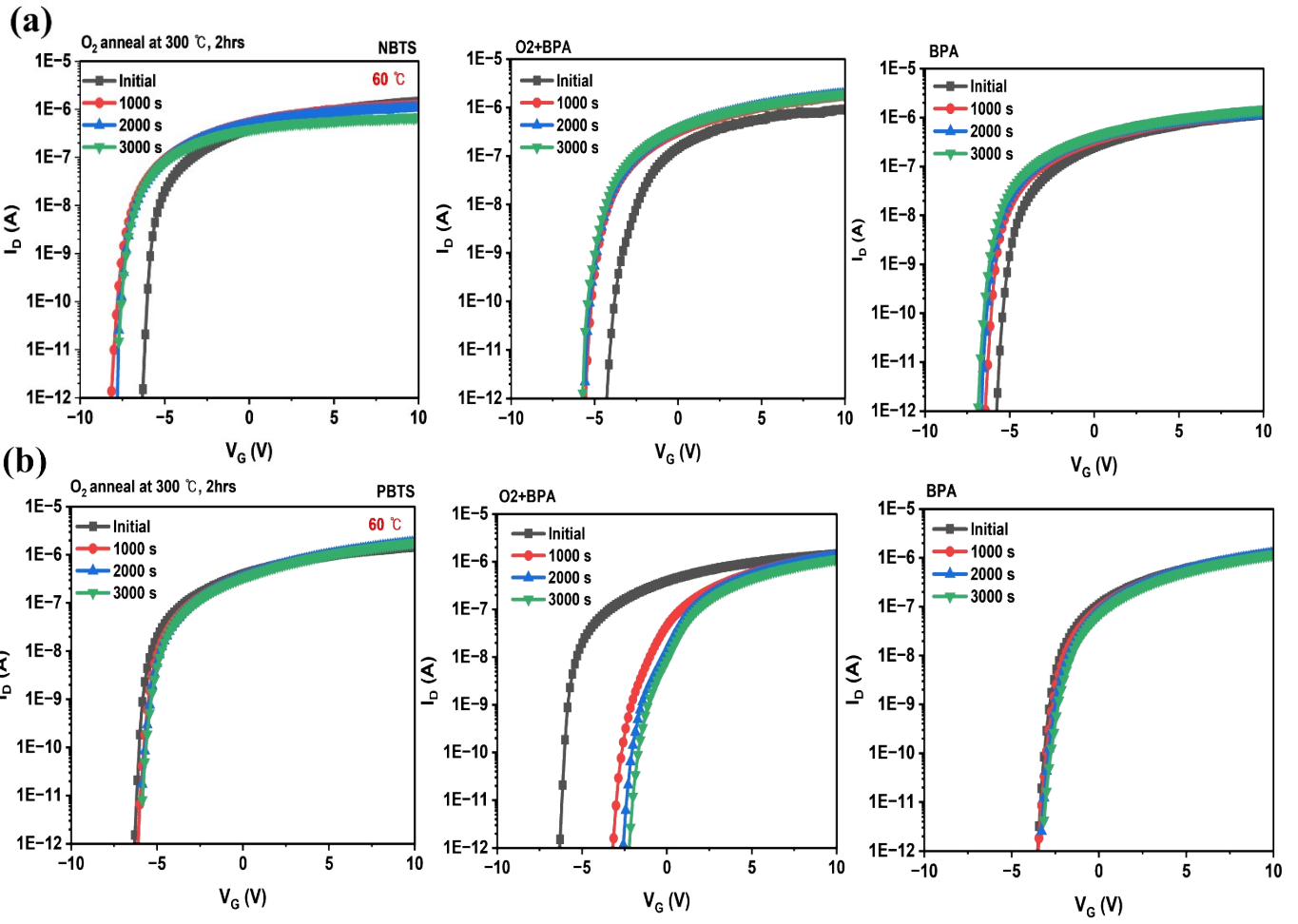
108

109

110

111

112



114

115

116

117 **Fig. S4.** This transfer curve shows the stability under thermal conditions at 60 °C. Positive and  
118 negative bias temperature stress (NBTS and PBTS).

119

120 Fig. S4 (a) shows the NBTS under 60 °C at  $V_G \pm 5$  V up to 3,000 sec. For the O<sub>2</sub> anneal In<sub>2</sub>O<sub>3</sub>  
121 TFT, the  $V_{th}$  shifted further in the negative direction, from -3.62 V initially to -6 V after 3,000  
122 sec. The O<sub>2</sub> anneal with BPA and BPA In<sub>2</sub>O<sub>3</sub> TFTs exhibited  $V_{th}$  values of -2.1 V and -0.4 V,  
123 respectively, after 3,000 sec. The stability of In<sub>2</sub>O<sub>3</sub> TFT is due to the back-channel layer of the  
124 ultra-thin In<sub>2</sub>O<sub>3</sub> film, which acts as the interfacial channel between the semiconductor and the  
125 insulator. This back channel is more dominant than the interfacial channel layer between the  
126 semiconductor and insulator, resulting in stable device characteristics with surface  
127 modification. The PBTS exhibits a similar trend to the NBTS measurement results. In the case  
128 of O<sub>2</sub> annealed In<sub>2</sub>O<sub>3</sub> TFT, the initial -3.3 V shifted significantly in the positive voltage  
129 direction to -1.24 V after 3,000 sec. However, the O<sub>2</sub> annealed In<sub>2</sub>O<sub>3</sub> TFTs with BPA  
130 passivation showed a larger positive voltage shift from an initial -3.3 V to 2.2 V after 3,000  
131 sec. The increase in electron carriers at the interface is due to the oxygen injected through O<sub>2</sub>  
132 annealed treatment inside the film, which results in more In-O bonds being broken and the  
133 oxygen becoming more In-O. For the BPA-only In<sub>2</sub>O<sub>3</sub> TFT, the  $V_{th}$  initially measures 0.35 V.  
134 As the existing carrier concentration remains constant, it shifts approximately 0.65 V in the  
135 positive direction. After 3,000 sec, the  $V_{th}$  value reaches 1 V, given that the initial  $V_{th}$  was 0.35  
136 V and the existing carrier concentration remained constant. The results indicate that aromatic  
137 rings with a chemically stable structure can maintain the  $V_{th}$  stability of In<sub>2</sub>O<sub>3</sub> TFT even in  
138 thermal environments.

139

140

141

142

143

144

145

146

147

148

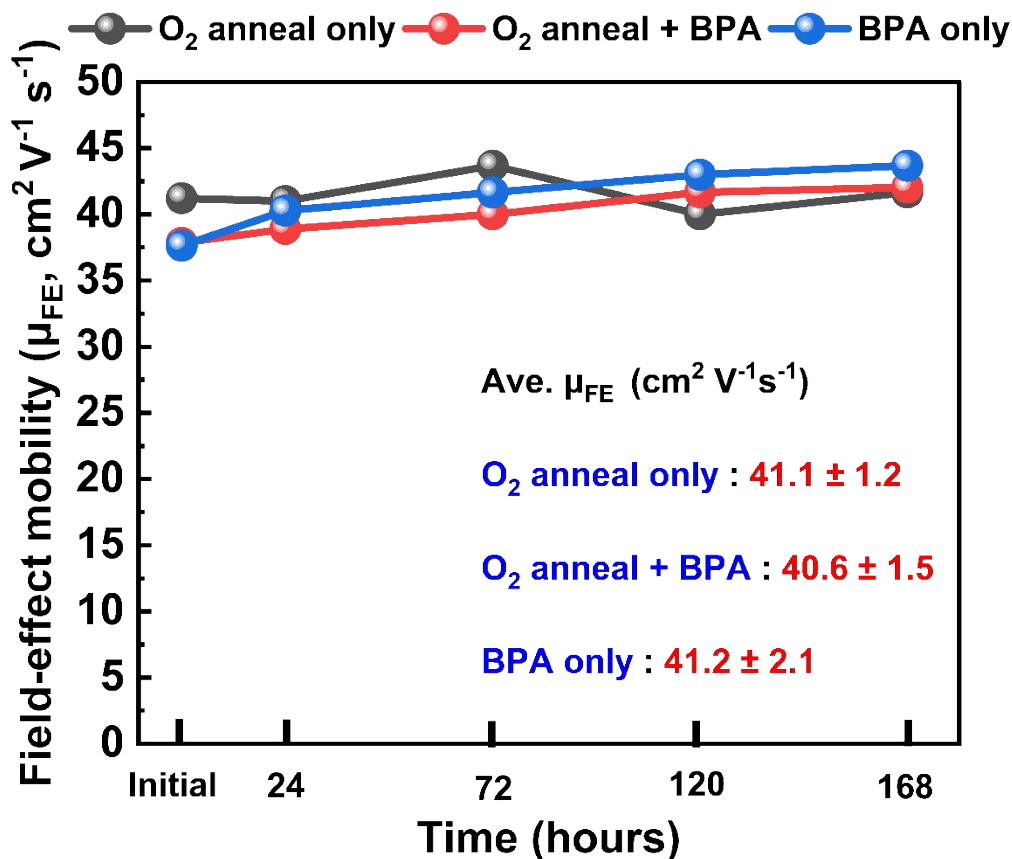
149

150

151

152

153



154 **Fig. S5.** This graph illustrates the temporal dependency of field-effect mobility in  $\text{In}_2\text{O}_3$  TFTs  
155 treated with  $\text{O}_2$  anneal,  $\text{O}_2$  anneal+BPA, and BPA. As the results, regardless of the treatment  
156 method and time intervals,  $\text{In}_2\text{O}_3$  TFTs exhibit non-varying mobility of  $41.1 \text{ cm}^2 \text{V}^{-1} \text{s}^{-1}$ ,  $40.6$   
157  $\text{ cm}^2 \text{V}^{-1} \text{s}^{-1}$ , and  $41.2 \text{ cm}^2 \text{V}^{-1} \text{s}^{-1}$  for the  $\text{O}_2$  anneal only,  $\text{O}_2$  anneal+BPA, and BPA only  
158 treatments, respectively.